A high temperature transition in $MgGeO_3$ from clinopyroxene ($C2/c$) type to orthopyroxene ($Pbca$) type

Takamitsu Yamanaka, Masahiro Hirano and Yoshio Takéuchi

Mineralogical Institute, Faculty of Science
University of Tokyo, Hongo, Tokyo 113 Japan

Abstract

X-ray diffraction studies of the transition of $MgGeO_3$ from monoclinic to orthorhombic symmetry at elevated temperatures have been conducted by precession photography on single-crystals of the polymorphs, which were synthesized by the flux method. The transition occurs rapidly as a topotactic transformation and obeys the following orientation relations of the orthorhombic (o) with respect to the monoclinic (c): $a_o//a_c^*$, $b_o//b_c$ and $c_o//c_c$. These structures are very similar to those of high-clinopyroxene (Cpx) and orthopyroxene (Opx), but the stability relation of the clino-form (low temperature) to the ortho-form (high temperature) is reversed in the germanate compared to the silicate pyroxenes. Both monoclinic ($a = 9.605(2)$, $b = 8.940(2)$, $c = 5.160(1)$Å, $\beta = 100.95(1)°$, $C2/c$) and orthorhombic ($a = 18.829(3)$, $b = 8.920(2)$, $c = 5.347(1)$Å, $Pbca$) $MgGeO_3$ structures were refined at temperatures up to 1100°C. At room temperature the clino-$MgGeO_3$ among $M^{2+}GeO_3$ (M^{2+} = Mg, Mn, Fe, Co) most closely approximates an ideal clinopyroxene structure, based on the cubic closest packing (CCP) of oxygen atoms, having $a/c = \sqrt{11/3}$, $c/b = \sqrt{3}/3$ and $\beta = 100.025°$. Increasing temperature gradually deforms this ideal structure. Under thermal expansion, bond distances vary inversely with ionic strength, and the volume expansion of Mg1 and Mg2 octahedra forces the chain of GeO_4-tetrahedra to straighten and tilt. A possible slip model of oxygen layers in the clino-to-ortho transition of $MgGeO_3$ is proposed for the topotactic transformation.

Introduction

The polymorphism of enstatite $MgSiO_3$ has been summarized by Smith (1969), and the aspects of the structure transition have been discussed by Sadanaga et al. (1969), Papike et al. (1973), Smyth (1974) and Murakami et al. (1982). Moreover studies on the phase relations of germanate pyroxenes have attracted attention owing to the analogy of these structures to those of silicate pyroxenes. Roth (1955) first reported the isotypism of $MgGeO_3$ with orthoenstatite. Robbins and Levin (1959) found another polymorph of $MgGeO_3$, analogous to clinoenstatite, but stable at higher temperature than ortho-$MgGeO_3$. Pyroxene-type polymorphs of other germanates, $MnGeO_3$, $CoGeO_3$ and $FeGeO_3$, have also been reported (Tauber et al., 1963; Tauber and Kohn, 1965; Royan and Forwerg, 1963; Grebenshchikov et al., 1976).

Ringwood and Seabrook (1963) and Ozima and Akimoto (1983) stated, in their study of high pressure and temperature phase transformation in $MgGeO_3$, that clino-$MgGeO_3$ is stable at higher pressure and lower temperature than ortho-$MgGeO_3$. This observation is at variance with the stability relation reported by Robbins and Levin (1959).

Peacor (1968) was the first to investigate the structure of $CoGeO_3$, which he found to be quite similar to that of high-clinoenstatite (Cpx), stating that the arrangement of oxygen atoms approximates a cubic closest packing (CCP).

The structure of orthorhombic $MgGeO_3$, refined by Fang et al. (1969), proved to be isostructural with orthoenstatite, and Hirano et al. (1980) found monoclinic $MnGeO_3$ to be isostructural with $CoGeO_3$ (Peacor, 1968).

We have synthesized single-crystals of both monoclinic and orthorhombic $MgGeO_3$ and refined their structures. We have also found, in our high temperature X-ray-diffraction studies, that the monoclinic phase (Cpx) with space group $C2/c$ transforms to the orthorhombic phase (Opx) with space group $Pbca$ at about 900°C by topotactic transformation. This type of clino-to-ortho transition at elevated temperatures has not been found in silicate pyroxenes. This paper presents refined structures of both clino- and ortho-$MgGeO_3$ at various temperatures up to 1100°C, discusses structural variations as a function of temperature and suggests a possible mechanism for the newly found transition in the pyroxene-type structures.

Preparation of single-crystals of clino- and ortho-$MgGeO_3$

Single-crystals of clino- and ortho-$MgGeO_3$ having stoichiometric composition were prepared from a mixture of reagent-grade powders of $MgCO_3$, MgF_2 and GeO_2 blended in the ratios 1:2:3. MgF_2 acts as a flux. Ortho-$MgGeO_3$ was prepared by keeping the mixture at 1550°C for 20 hrs before quenching it to room temperature. The crystals thus obtained are transparent and prismatic, up to
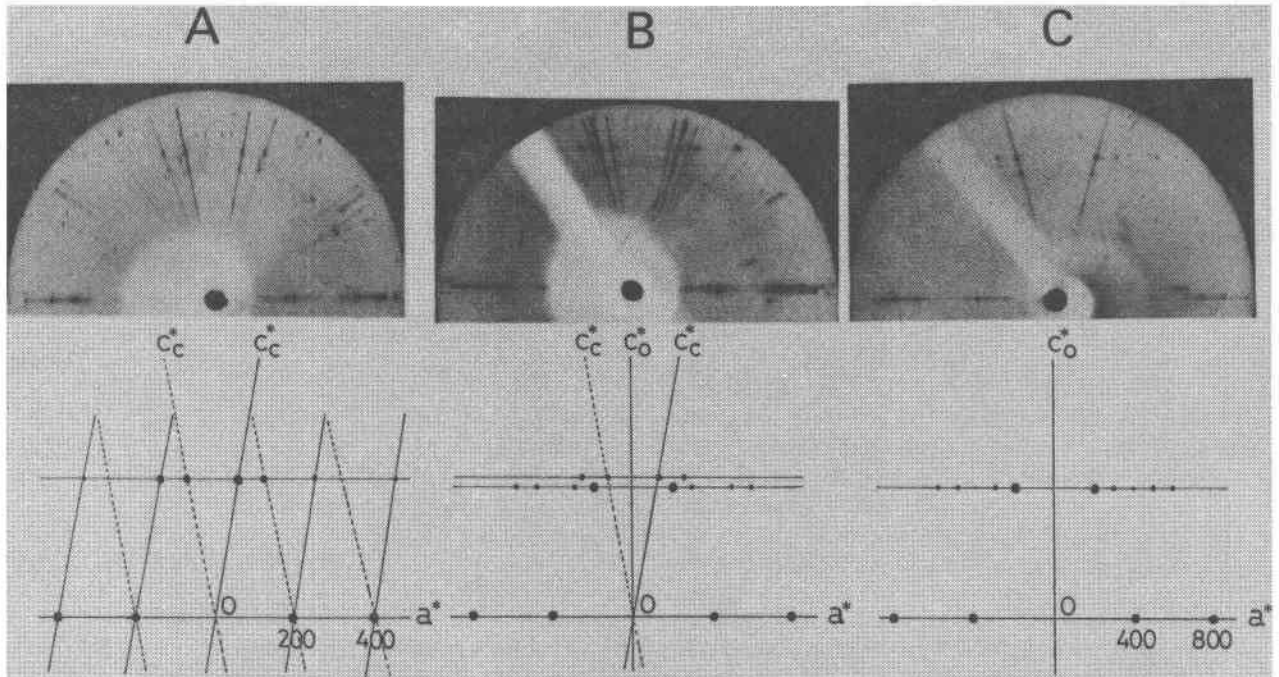
Fig. 1.   The $h0l$ precession photographs (MoKα unfiltered, $\mu = 10°$) of the MgGeO$_3$ crystal, showing the process of the topotactic from clino- to ortho-phase. (A) Diffraction pattern of the twinned clino-phase at 800°C. (B) After heating the sample at 900°C for 30 min, showing patterns of the twinned clino-phase and the ortho-phase with common a* axis. (C) After further heating for one hour, exhibiting the single pattern of the inverted ortho-phase.

$0.3 \times 0.1 \times 0.1$ mm in size. They are commonly euhedral and elongated parallel to **c**. Crystals of clino-MgGeO$_3$ were synthesized with the starting mixture heated at 1360°C and then slowly cooled to 800°C at the rate of 4°C/hr; they usually grow to approximately the same size as those of ortho-MgGeO$_3$ and are likewise euhedral. To insure homogeneity and stoichiometry, both samples were tested with EPMA. A few stacking faults were detected in the ortho-phase by means of TEM lattice images.

Observation of the topotactic transition of clino-MgGeO$_3$

The clino-to-ortho transition in MgGeO$_3$ was investigated by means of X-ray-precession photographs at elevated temperatures. A fragment of a clino-MgGeO$_3$ crystal was set on the head of a thermocouple, mounted on the goniometer head, and the sample was heated to the desired temperatures by electric micro-heater and gas flame heater (Yamanaka et al., 1981). The methods to measure the temperature, by both thermocouple and optical pyrometer, are described elsewhere (Murakami et al., 1982).

Precession photographs were taken (MoKα, 140 mA, 50 kV, $\mu = 10°$) after each 30-minute heating period. All the tested samples of the clino-phase showed a twinned pattern with twin-and-composition plane (100) (Fig. 1A). No changes in the diffraction pattern of $h0l$ of the clino-phase were observed at temperature up to 800°C. After heating the sample for 30 minutes at 900°C, reciprocal lattice row

$h02$ showed both clino and ortho patterns (Fig. 1B). This fact and additional photographs prove that the clino-phase ($C2/c$) is transformed to the ortho-phase ($Pbca$) and that the transition is topotactic obeying the following relations: $\mathbf{a}_o//\mathbf{a}_c^*$, $\mathbf{b}_o//\mathbf{b}_c$, $\mathbf{c}_o//\mathbf{c}_c$. The $h02$ reflections of the clino-phase show diffuse streaks parallel to a*, indicating the existence of a disordered stacking sequence parallel to [100]. After heating for another 30 minutes at same temperature, neither clino-phase reflections nor diffuse streaks were seen on the photograph: only the sharp reflections of the ortho-phase were observed (Fig. 1C). These observations indicate that the clino-phase first changes from its ordered stacking sequence to the disordered one during the transition, after which it is transformed to the ortho-phase, having a well ordered sequence, different from that of the clino-phase. At 1000°C the clino-phase is rapidly transformed into the ortho-phase. No observation above 1200°C could be performed, because of the sublimation of the specimen. Thus, the existence of other possible polymorphs, similar in structure to protoenstatite, could be confirmed.

After heating a crystal of ortho-MgGeO$_3$ for 24 hours at 700°C in order to induce the reverse transformation from ortho- to clino-phase, we found that the diffraction pattern of the ortho-phase remained unchanged. This observation demonstrates that the reverse transformation proceeds sluggishly, if at all, at the annealing temperture. The present *in situ* experiment of the transformation at elevated temperatures could not establish the exact transition tem-

perature, but it did confirm the stability relation of the two polymorphs: the clino-phase is the low temperature form and the ortho-phase the high temperature form. None of the silicate pyroxenes reported to date have shown this type of transition.

Refinement of the structures

A fragment of the clino-$MgGeO_3$ crystal $0.20 \times 0.08 \times 0.08$ mm in size, was used for the structure refinements. Unit-cell dimensions at elevated temperatures were determined by least squares refinement from 2θ values of 25 reflections within the range $40° < 2\theta < 55°$ (Table 1). The determination was made on a RIGAKU-AFC5 diffractometer with graphite-monochromated $MoK\alpha$ radiation ($\lambda = 0.71069Å$) from a rotating anode generator (160 mA, 50 kV). Diffraction-intensity measurements were made at 20, 210, 420, 620 and 750°C for clino-$MgGeO_3$ and at 20, 950 and 1100°C for ortho-$MgGeO_3$, with a micro-electric heater set on the χ-circle and gas-flame heater. X-ray-diffraction intensities were measured by employing the ω-2θ scanning mode; the scanning speed was $10°$/min in 2θ and the scanning width, $1.2 + 0.5°$ tan θ. The intensities greater than $3\sigma|F|$ were corrected for Lorentz and polarization factors and a transmission factor. The full matrix least-squares refinements, including anisotropic temperature factors and isotropic extinction parameter, were conducted by means of the program LINUS (Coppence and Hamilton, 1970). Atomic scattering factors and anomalous dispersion parameters were taken from the *International Table for X-ray Crystallography, Vol. III* (1974). The structure parameters obtained from the refinement at each temperature are presented in Table 2. The number of reflections observed and used and the final residuals (R and R_{wt}) of each refinement are listed in Table 1.

Since all the samples of clino-$MgGeO_3$ that were tested by precession photography turned out to be twins, the specimen chosen for the refinement was the one having the largest volume ratio of the two individual crystals in the twin. Only $hk0$ reflections within the 70° range in 2θ ($MoK\alpha$) were superposed by the twinned crystals. Consequently, the reflections were divided into two groups: $hk0$ reflections and other-than-$hk0$ reflections. Two different scale factors were then employed in the least squares refinement. An average intensity ratio of 25 reflection pairs having the same indices was adopted as an initial value of the scale factor. The volume ratio of the individual crystals in the twin was estimated to be 26.7:1 from the converged scale factors of the two sets of the intensities obtained at room temperature. The structure refinements at high temperatures were conducted in the same manner as that at room temperature described above.

Structures of clino- and ortho-$MgGeO_3$ at room temperature

Clino-$MgGeO_3$

The structure of clino-$MgGeO_3$ (Table 3a) was found to be analogous to that of clino-$CoGeO_3$ (Peacor, 1968). The arrangement of the oxygen atoms approximates a cubic closest packing (CCP), as reported by Peacor (1968), and tetrahedra and octahedra formed by the oxygen atoms are close to regular polyhedra (Fig. 2). Unit-cell parameters (Table 4) prove that, in comparison to clino-phases of $CoGeO_3$, $MnGeO_3$ and $FeGeO_3$, clino-$MgGeO_3$ more closely approximates CCP of oxygen atoms. In this ideal structure composed of CCP oxygen, if r denotes the ionic radius of oxygen, the unit-cell parameters are expressed by $a = 2\sqrt{11}r$, $b = 6r$, $c = 2\sqrt{3}r$, and $\beta = 100.025°$.

Silicate pyroxenes such as diopside-type clinopyroxene and high-clinopyroxene having space group $C2/c$, show considerable distortion from CCP. Compared with the germanate pyroxenes, the smaller tetrahedral chain bridging the octahedral bands in the silicate pyroxenes requires larger cations such as Ca or Na in the M2 sites, whereas

Table 1. Unit-cell parameters and factors of refinements

	Clino-MgGeO₃					Ortho-MgGeO₃		
	20°C	210°C	420°C	620°C	750°C	20°C	950°C	1100°C
$a(Å)$	9.605(2)	9.640(2)	9.659(2)	9.686(1)	9.706(3)	18.829(3)	19.011(5)	19.031(7)
$a\sin\beta$	9.431(2)	9.458(2)	9.474(2)	9.496(1)	9.509(3)			
$b(Å)$	8.940(2)	8.978(2)	8.992(2)	9.024(2)	9.040(3)	8.952(2)	9.084(2)	9.110(3)
$c(Å)$	5.160(1)	5.173(1)	5.180(1)	5.192(1)	5.202(1)	5.347(1)	5.415(2)	5.428(4)
β	100.95(1)	101.14(1)	101.23(1)	101.38(1)	101.56(3)			
a/b	1.0744	1.0737	1.0742	1.0733	1.0737	1.9916	2.0928	2.0891
c/b	0.5772	0.5762	0.5761	0.5753	0.5754	0.5972	0.5961	0.5975
$V(Å^3)$	435.1(1)	439.2(1)	441.3(1)	444.9(1)	447.1(3)	901.3(3)	935.2(5)	941.0(8)
$Dx(g/cm^3)$	4.424	4.382	4.361	4.326	4.304	4.271	4.116	4.090
$\theta_{max}(°)$	70	60	60	60	60	100	55	
N obs.	959	645	652	649	653	3716	1144	
N used	826	545	554	499	500	1838	589	
R(%)	3.58	4.65	4.96	5.21	3.76	5.21	11.55	
$R_{wt}(\%)$	3.92	5.95	6.03	6.27	4.54	6.25	12.60	

Parenthesized figures represent the estimated standard deviation (esd) and refer to the last decimal place. This notation for esd is used consistently throughout this work.

Table 2a.   Atomic coordinates of clino-MgGeO$_3$

		20°C	210°C	420°C	620°C	750°C
Mg1	x	0.0	0.0	0.0	0.0	0.0
	y	.9071(3)	.9068(5)	.9062(5)	.9062(6)	.9047(6)
	z	.25	.25	.25	.25	.25
	β_{11}	.0012(2)	.0030(4)	.0039(5)	.0052(6)	.0057(4)
	β_{22}	.0012(2)	.0028(5)	.0028(5)	.0045(6)	.0057(4)
	β_{33}	.0050(6)	.0102(15)	.0106(15)	.0156(18)	.0155(13)
	β_{13}	-.0002(3)	-.0003(6)	-.0002(6)	-.0004(8)	.0003(6)
Mg2	x	0.0	0.0	0.0	0.0	0.0
	y	.2700(3)	.2704(5)	.2705(5)	.2709(6)	.2700(5)
	z	.25	.25	.25	.25	.25
	β_{11}	.0014(2)	.0035(5)	.0044(5)	.0061(6)	.0068(5)
	β_{22}	.0014(2)	.0031(5)	.0034(5)	.0049(6)	.0058(5)
	β_{33}	.0044(6)	.0110(16)	.0108(16)	.0167(20)	.0128(17)
	β_{13}	-.0005(3)	-.0004(7)	.0002(7)	-.0001(9)	.0001(5)
Ge	x	.3002(1)	.2999(1)	.2997(1)	.2994(1)	.2993(1)
	y	.0945(1)	.0944(1)	.0944(1)	.0944(1)	.0944(1)
	z	.2108(1)	.2117(1)	.2121(2)	.2127(1)	.2127(2)
	β_{11}	.0009(1)	.0021(1)	.0027(1)	.0035(1)	.0035(1)
	β_{22}	.0010(1)	.0025(1)	.0027(1)	.0041(1)	.0046(1)
	β_{33}	.0039(3)	.0104(4)	.0094(4)	.0151(2)	.0129(2)
	β_{12}	-.0001(1)	-.0001(1)	-.0001(1)	-.0001(1)	-.0001(1)
	β_{13}	-.0007(1)	-.0002(1)	.0001(1)	-.0003(1)	.0015(1)
	β_{23}	-.0000(1)	-.000 (2)	-.0001(2)	-.0001(2)	.0001(2)
O1	x	.1160(3)	.1166(6)	.1164(7)	.1166(8)	.1157(5)
	y	.0909(4)	.0906(7)	.0911(8)	.0906(9)	.0923(8)
	z	.1325(6)	.1324(13)	.1337(13)	.1319(16)	.1332(11)
	β_{11}	.0033(2)	.0024(6)	.0030(6)	.0038(8)	.0041(5)
	β_{22}	.0013(3)	.0038(7)	.0034(7)	.0060(10)	.0062(7)
	β_{33}	.0065(10)	.0100(12)	.0146(22)	.0220(27)	.0165(20)
	β_{12}	-.0001(2)	-.0001(6)	-.0003(6)	.0001(6)	-.0012(6)
	β_{13}	-.0006(4)	-.0010(10)	-.0006(12)	-.0009(11)	.0011(8)
	β_{23}	.0005(5)	.000 (12)	-.0002(11)	-.0002(15)	-.0026(11)
O2	x	.3826(3)	.3828(7)	.3831(7)	.3833(8)	.3813(6)
	y	.2435(4)	.2427(7)	.2421(8)	.2418(9)	.2418(7)
	z	.3814(6)	.3806(11)	.3817(13)	.3814(16)	.3839(11)
	β_{11}	.0012(2)	.0036(7)	.0043(7)	.0053(9)	.0065(7)
	β_{22}	.0013(3)	.0029(7)	.0036(8)	.0047(9)	.0042(7)
	β_{33}	.0049(9)	.0115(24)	.0098(22)	.0185(29)	.0151(20)
	β_{12}	-.0005(2)	-.0011(6)	-.0012(6)	-.0014(7)	-.0013(5)
	β_{13}	-.0006(4)	-.0026(6)	-.0021(10)	-.0017(13)	.0004(10)
	β_{23}	-.0001(4)	-.0012(11)	-.0013(10)	-.0017(13)	-.0001(10)
O3	x	.3601(3)	.3601(7)	.3599(7)	.3588(8)	.3673(7)
	y	.0688(3)	.0682(7)	.0686(7)	.0677(8)	.0680(7)
	z	.9034(6)	.9057(14)	.9050(13)	.9088(16)	.9091(12)
	β_{11}	.0016(3)	.0025(6)	.0029(6)	.0047(8)	.0060(7)
	β_{22}	.0014(3)	.0027(7)	.0033(7)	.0046(9)	.0075(9)
	β_{33}	.0040(9)	.0145(26)	.0144(24)	.0201(20)	.0181(22)
	β_{12}	-.0006(2)	-.0008(6)	-.0008(6)	-.0016(7)	-.0011(6)
	β_{13}	.0001(4)	.0007(10)	.0014(10)	.0010(13)	.0036(10)
	β_{23}	-.0008(4)	-.0017(10)	-.0017(11)	-.0021(14)	-.0030(11)

Table 2b.   Atomic coordinates of ortho-MgGeO$_3$

		20°C	950°C
Mg1	x	0.1232(2)	0.1237(7)
	y	.3440(3)	.3647(16)
	z	.3503(5)	.3565(24)
	B_{iso}	.55(6)	2.66(22)
Mg2	x	.3774(3)	.3776(7)
	y	.4890(5)	.4874(16)
	z	.3443(9)	.3532(28)
	B_{iso}	.51(7)	2.97(25)
Ge A	x	.2709(1)	.2710(17)
	y	.3454(2)	.3450(39)
	z	.0408(2)	.0422(64)
	B_{iso}	.35(1)	1.56(5)
Ge B	x	.4722(1)	.4729(2)
	y	.3393(2)	.3387(4)
	z	.8055(2)	.8035(6)
	B_{iso}	.37(1)	1.74(5)
O1 A	x	.1787(4)	.1771(11)
	y	.3409(13)	.3347(27)
	z	.0188(14)	.0250(44)
	B_{iso}	.37(9)	2.04(41)
O2 A	x	.3119(5)	.3093(13)
	y	.5132(10)	.5150(31)
	z	.0382(18)	.0437(56)
	B_{iso}	.63(11)	3.04(54)
O3 A	x	.3071(5)	.3069(14)
	y	.2104(11)	.2141(30)
	z	.8337(17)	.8324(60)
	B_{iso}	.80(15)	3.32(56)
O1 B	x	.5636(4)	.5667(13)
	y	.3362(13)	.3415(32)
	z	.8147(16)	.8090(56)
	B_{iso}	.56(11)	3.07(49)
O2 B	x	.4299(4)	.4289(12)
	y	.4863(11)	.4852(27)
	z	.6689(19)	.6791(53)
	B_{iso}	.60(12)	2.32(45)
O3 B	x	.4455(4)	.4481(10)
	y	.1794(8)	.1745(23)
	z	.6259(15)	.6290(37)
	B_{iso}	.34(11)	1.08(34)

the M1 site generally contains a smaller cation than M2. The distortion from CCP results from the size difference between M1 and M2 sites. In the clino-MgGeO$_3$ structure, large Ge-tetrahedral chains conform to CCP of oyxgen atoms and result in the ideal octahedra in M1 and M2 sites, which correspond to Mg1 and Mg2, respectively.

The O3′–O3–O3″ angle has been discussed as a parameter of the chain geometry, particularly its "straightness" or its "kink", because O3 is the bridging oxygen atom of adjacent tetrahedra. This angle is closer to the ideal value of 120° in MgGeO$_3$ (129.03°) than in other germanate pyroxenes: 133.4° in CoGeO$_3$ (Peacor, 1968), 135.1° in MnGeO$_3$ (Hirano et al., 1980); and considerably more so than in silicate pyroxenes: diopside (166.4°), jadeite (174.6°) (Cameron et al., 1973). The angle of Ge–O3–Ge′ in clino-MgGeO$_3$ is 117.95°, which is similar to the ideal angle of 109.47°, as compared to Si–O3–Si′ in the silicate tetrahedral chain. Two bridging bonds, Ge–O3 (1.801Å) and Ge–O3′ (1.798Å) are significantly longer than two non-bridging bonds; Ge–O1 (1.738Å) and Ge–O2 (1.706Å). The acentric location of Ge ions in the tetrahedron is caused by

the effect of the electrostatic valency differences in oxygen atoms. One way in which clino-MgGeO$_3$ differs from silicate pyroxenes is that its structure shows no shared edges between octahedra and tetrahedra. The above features demonstrate that Ge–O bonds have a stronger ionic (less covalent) character than Si–O bonds.

Ortho-MgGeO$_3$

The lattice parameters obtained from single crystals of ortho-MgGeO$_3$ (Table 4) are similar to those derived from powder data (Roth, 1955); they are all a little larger than those of orthoenstatite (Smith, 1969) but smaller than those of other germanate orthopyroxenes, MnGeO$_3$ (Fang et al., 1969) and CoGeO$_3$ (Tauber et al., 1965).

Interatomic distances and angles of ortho-MgGeO$_3$ at 20°C (Table 3) indicate that its structure is very similar to that of ortho-MgGeO$_3$ (Fang et al., 1969). The structure (Fig. 3) is made up of four pairs of alternating tetrahedral and octahedral layers parallel to (100). There are two crystallographically distinct tetrahedral chains, the A chain and

Table 3a. Interatomic distances, volumes of the polyhedra and tetrahedral chain angles

Atoms	Clino-MgGeO$_3$					Ortho-MgGeO$_3$	
	20°C	210°C	420°C	620°C	750°C	20°C	950°C
Mg1 - O1 A (A) }	2.137(3)	2.150(8)	2.159(8)	2.167(9)	2.186(8)	2.057(8)	2.215(32)
O1 B						2.154(11)	2.141(28)
O1 A'	2.074(3)	2.078(6)	2.084(6)	2.080(7)	2.083(5)	2.154(11)	2.112(32)
O1 B' }						2.115(9)	2.065(27)
O2 A }	2.040(4)	2.049(8)	2.055(8)	2.061(9)	2.074(7)	2.033(10)	2.061(29)
O2 B						2.062(11)	2.055(31)
Mean	2.084(3)	2.092(7)	2.099(8)	2.102(8)	2.115(7)	2.096(10)	2.108(29)
σ	0.0402	0.0425	0.0438	0.0461	0.0508	0.0478	0.0569
V (Å^3)	11.776	11.921	12.022	12.089	12.285	12.048	12.159
Mg2 - O1 A }	2.104(3)	2.122(7)	2.119(7)	2.139(8)	2.117(7)	2.075(13)	2.077(38)
O1 B						2.099(14)	2.135(34)
O2 A }	2.023(3)	2.027(7)	2.022(7)	2.025(8)	2.022(5)	1.997(13)	2.016(39)
O2 B						2.061(13)	2.135(39)
O3 A }	2.217(3)	2.233(7)	2.234(7)	2.262(8)	2.282(7)	2.223(14)	2.331(32)
O3 B						2.298(12)	2.273(36)
Mean	2.115(3)	2.127(7)	2.125(7)	2.142(8)	2.140(6)	2.125(13)	2.161(36)
σ	0.0796	0.0842	0.0867	0.0967	0.1074	0.1026	0.1087
V (Å^3)	12.393	12.610	12.577	12.862	12.848	12.180	12.669
Ge - O1 B	1.739(3)	1.735(6)	1.738(7)	1.738(7)	1.746(5)	1.723(8)	1.784(26)
GeB O2 B	1.706(3)	1.704(6)	1.705(7)	1.708(8)	1.708(6)	1.702(9)	1.711(28)
O3 B	1.798(3)	1.803(7)	1.806(7)	1.810(8)	1.813(6)	1.796(8)	1.828(20)
O3 B'	1.801(3)	1.804(8)	1.812(8)	1.799(9)	1.796(7)	1.793(8)	1.827(21)
Mean	1.761(3)	1.762(7)	1.765(7)	1.764(8)	1.766(6)	1.753(8)	1.788(23)
σ	0.0402	0.0434	0.0454	0.0423	0.0416	0.0417	0.04761
V (Å^3)	2.735	2.736	2.753	2.741	2.753	2.753	2.901
GeA - O1 A						1.741(6)	1.789(22)
O2 A						1.689(9)	1.708(28)
O3 A						1.775(10)	1.781(30)
O3 A'						1.779(9)	1.796(32)
Mean						1.746(9)	1.768(28)
σ						0.0361	0.0353
V (Å^3)						2.644	2.754
Tetrahedral bond angles							
O3 A - Ge A - O3 A' (°)						102.20	102.26
O3 B - Ge B - O3 B'	105.15	105.02	104.94	105.31	105.74	111.00	112.23
Ge A - O3 A - Ge A'						126.40	127.70
Ge B - O3 B - Ge B'	117.95	118.05	117.78	118.71	119.11	120.49	119.07
O3 A'- O3 A - O3 A"						150.32	152.93
O3 B'- O3 B - O3 B"	129.03	129.30	129.07	129.59	129.40	129,37	126.29

the B chain, both of which have an O rotation (Thompson, 1970). The A chain looks a little more stretched than the B chain, as a result of a large O3A'–O3A–O3A" angle (150.32°). Each tetrahedron in the A chain shares one edge with the M2 octahedron. The B chain in ortho-MgGeO$_3$ is little different from the chain in clino-MgGeO$_3$. As to the angles O3B'–O3B–O3B" and GeB–O3B–GeB', they are 129.37° and 120.49°, respectively, in ortho-MgGeO$_3$ versus 120.37° and 117.95° in clino-MgGeO$_3$. The GeB tetra-

hedron is larger and more regular than the GeA tetrahedron.

As mentioned above, the M2 octahedron shares an edge with the GeA-tetrahedron. It follows that the octahedron is extremely distorted. Mg2-O3A and Mg2-O3B bond lengths are more extended than the four other bonds in the M2 site. The volume of the M2 octahedron is a little larger than that of M1. The above features closely resemble those observed in orthoenstatite.

Table 3b. Lengths of edges in the polyhedra

	Clino-MeGeO$_3$					Ortho-MgGeO$_3$	
	20°C	210°C	420°C	620°C	750°C	20°C	950°C
Mg1 site							
O1A – O1A' }	3.049(5)	3.056(9)	3.065(10)	3.068(11)	3.090(9)	3.129(12)	3.177(42)
O1B – O1B'						3.087(13)	3.114(34)
O1A – O1B'	2.732(5)	2.756(10)	2.750(10)	3.068(11)	3.090(9)	2.807(10)	2.771(36)
O1A – O1B }	2.885(4)	2.897(9)	2.907(9)	2.904(10)	2.916(8)	2.830(12)	2.788(36)
O1A'– O1B'						2.830(12)	2.788(36)
O1A – O2B }	3.107(4)	3.124(10)	3.140(10)	3.148(11)	3.170(10)	3.189(14)	3.238(38)
O1B'– O2A						3.074(13)	2.918(37)
O1A'– O2B }	3.039(5)	3.047(10)	3.063(10)	3.064(11)	3.085(9)	3.188(14)	3.189(40)
O1B'– O2A						2.941(15)	3.134(38)
O1A'– O2A }	2.792(4)	2.808(9)	2.809(9)	2.815(11)	2.815(8)	2.817(12)	2.810(37)
O1B – O2B						2.687(12)	2.725(33)
O2A – O2B	2.844(5)	2.847(11)	2.858(11)	2.861(13)	2.922(9)	2.982(13)	3.022(37)
Mean	2.944(4)	2.955(9)	2.965(10)	2.969(11)	2.986(9)	2.959(12)	2.973(37)
σ	0.1266	0.1279	0.1335	0.1312	0.1392	0.1456	0.1841
Mg2 site							
O1A – O1B	2.732(5)	2.756(10)	2.750(10)	2.775(11)	2.760(8)	2.807(11)	2.772(36)
O1A – O2B }	2.910(5)	2.929(10)	2.923(10)	2.945(11)	2.921(9)	2.687(12)	3.078(40)
O1B – O2A						2.817(13)	2.954(38)
O1A – O2A }	2.792(4)	2.807(9)	2.809(9)	2.815(10)	2.815(8)	2.888(13)	2.810(37)
O1B – O2B						3.037(14)	2.725(33)
O1A – O3A }	3.059(4)	3.080(9)	3.078(10)	3.103(11)	3.093(10)	3.465(15)	3.057(36)
O1B – O3B						3.093(14)	3.614(38)
O2A – O3A }	2.957(4)	2.960(9)	2.958(10)	3.103(11)	3.093(10)	2.552(14)	3.139(33)
O2B – O3B						3.274(13)	3.488(38)
O2A – O3B }	3.157(5)	3.180(10)	3.173(10)	3.206(12)	3.200(10)	3.086(12)	2.604(41)
O2B – O3A						3.415(13)	3.334(34)
O3A – O3B	3.369(5)	3.398(11)	3.404(10)	3.460(12)	3.500(10)	2.847(12)	2.923(33)
Mean	2.988(4)	3.005(10)	3.003(10)	3.026(11)	3.026(9)	2.997(13)	3.042(37)
σ	0.1754	0.1786	0.1793	0.1908	0.1997	0.2715	0.2978
Ge (GeB) site							
O1B – O2B	2.969(4)	2.971(9)	2.972(9)	2.982(10)	2.970(8)	2.956(12)	3.013(35)
O1B – O3B	2.871(4)	2.874(9)	2.878(9)	2.877(10)	2.883(9)	2.817(12)	2.847(33)
O1B – O3B'	2.826(5)	2.826(10)	2.839(11)	2.821(12)	2.828(8)	2.780(12)	2.887(33)
O2B – O3B	2.805(4)	2.805(9)	2.807(10)	2.809(11)	2.815(9)	2.773(12)	2.859(34)
O2B – O3B'	2.892(4)	2.886(10)	2.892(10)	2.884(12)	2.897(9)	2.873(13)	2.859(32)
O3B – O3B'	2.858(4)	2.862(10)	2.869(10)	2.869(12)	2.877(9)	2.766(13)	3.035(29)
Mean	2.858(4)	2.871(10)	2.867(10)	2.874(11)	2.878(9)	2.838(12)	2.917(33)
σ	0.0528	0.0525	0.0512	0.0559	0.0505	0.0765	0.2978
GeA site							
O1A – O2A						2.946(12)	3.001(35)
O1A – O3A						2.861(12)	2.895(36)
O1A – O3A'						2.982(12)	3.001(36)
O2A – O3A						2.924(14)	2.963(41)
O2A – O3A'						2.552(14)	2.604(41)
O3A – O3A'						2.766(13)	2.786(46)
Mean						2.834(13)	2.876(39)
σ						0.1456	0.1437

High temperature crystal chemistry of MgGeO₃

A series of refinements at elevated temperatures reveal distinctive high-temperature behaviors of germanate pyroxene structures and provide insight into the behavior of analogous silicate pyroxenes.

Lattice parameters determined at high temperatures (Table 1) are plotted as a function of temperature in Figure 4. The cell edges, a_c, b_c and c_c of the clino-phase, increase linearly within the stable temperature range, with nearly equal thermal expansion coefficients. The β-angle function, however, is not linear: it has a positive curvature as temperature exceeds 500°C. The distance $a_c \sin \theta$, which is measured perpendicular to the octahedral bands, and has a value of about $a_o/2$ of the ortho-phase, varies linearly. Values of a_c, b_c and c_c change discontinuously to the corresponding a_o, b_o and c_o of the ortho-phase near 900°C, as the structure transition from clino- to ortho-phase takes
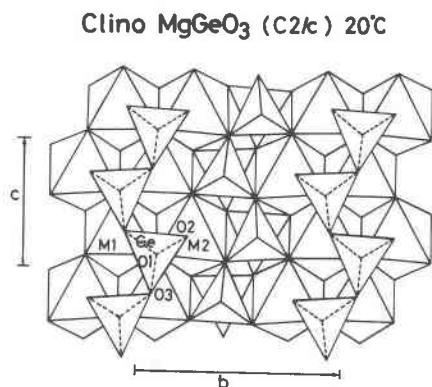
Clino MgGeO$_3$ (C2k) 20°C

Fig. 2. The clinopyroxene-type structure of $MgGeO_3$ at 20°C viewed along **a***.

Ortho MgGeO$_3$ (Pbca) 20°C

Fig. 3. First and second layers of the orthopyroxene-type structure of $MgGeO_3$ at 20°C viewed along **a***.

place. The value of c_c abruptly increases to that of c_o, while that of $a_c \sin \theta$ contracts to that of $a_o/2$, at the transition temperature. The remarkable expansion of c_o results from the great extension of the A chain in the ortho-phase. A comparison with the ideal values of a/b, c/b and β, of the values observed in the clino-structure at the various temperatures suggests that the oxygen atoms in the structure gradually depart from CCP as the temperature increases.

Interatomic distances and volumes of the cation tetrahedra and octahedra as a function of temperature (Table 3a) and lengths of O–O edges in the polyhedra (Table 3b) indicate the thermal effects on the clino- and ortho-$MgGeO_3$ structures. Mean distances of Mg1–O and

Mg2–O in the clino-structure (Fig. 5) increase linearly with temperature; the former is smaller than the latter, but their thermal expansion coefficients are almost equal. The volume increments of the Mg1 and Mg2 octahedra are also nearly equal. In contrast, the increment of the mean Ge–O distance and especially that of the volume of the tetrahedron are so small as to be within experimental errors. These thermal changes are consistent with those of silicate clinopyroxenes (Cameron et al., 1973).

The thermal expansion of the octahedra results in: (1) straightening of the tetrahedral chain; (2) tilting of the tetrahedra against the plane of the octahedral bands; (3) rotation of the tetrahedra. Since the bridging oxygen O3 in the tetrahedral chain links the Mg2 octahedron to the chain (Fig. 2), the extreme expansion of Mg2–O3 brings about the straightening of the chain by causing the angle of O3'–O3–O3" to increase with temperature.

The standard deviation σ of the interatomic distance, expressed by $\sigma = \Sigma(x - \overline{x})^2/n$, is regarded as a measure of the deformation of the regular polyhedron. The values of σ of Mg1–O, Mg2–O and O–O increase with temperature (Table 3a and Table 3b), suggesting a gradual deformation from the ideal structure. This feature is consistent with the variation of the unit-cell parameters with temperature.

The oxygen atom O1 being tetrahedrally coordinated with two Mg1's, Mg2, and Ge, has a valence sum of 2.0. Both O2 and O3 have coplanar three-fold coordinations, the former is coordinated by Mg1, Mg2, and Ge and the
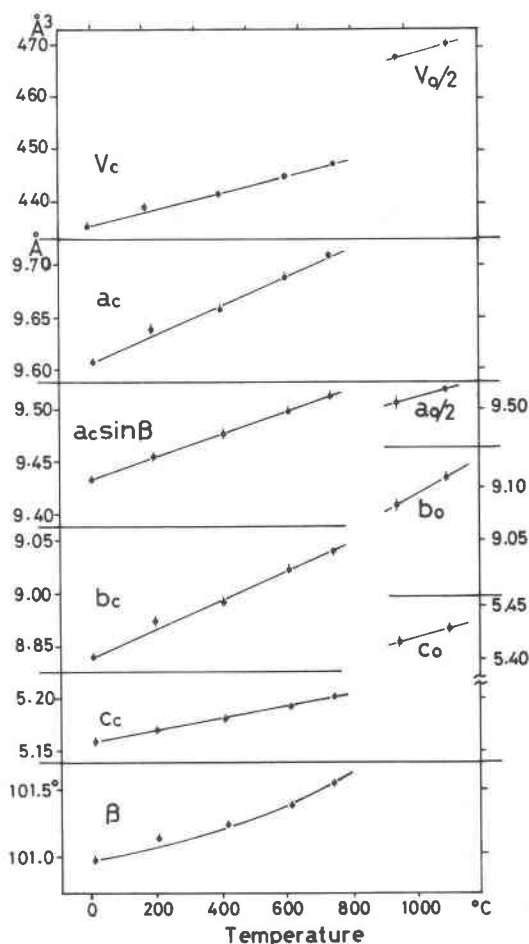
Table 4. Unit-cell parameters of germanate pyroxenes

Clinopyroxene (C2/c)

	MgGeO$_3$[1]	CoGeO$_3$[2]	FeGeO$_3$[3]	MnGeO$_3$[4]	ideal (r = 1.38 Å)[5]
a (Å)	9.605(2)	9.692(4)	9.798(1)	9.9204(9)	$2\sqrt{11}$ r = 9.154
b (Å)	8.940(2)	9.018(3)	9.150(1)	9.2779(6)	6 r = 8.280
c (Å)	5.160(1)	5.181(2)	5.196(1)	5.2765(5)	$2\sqrt{3}$ r = 4.781
β	100.34(1)°	101.2(1)°	101.84(1)°	101.74(1)°	100.025°
a/b	1.0743	1.0747	1.0708	1.0693	$\sqrt{11}/3$ = 1.1055
c/b	0.5772	0.5745	0.5679	0.5687	$1/\sqrt{3}$ = 0.5774
V (Å^3)	435.88(14)	444.00(25)	455.92(12)	475.50(7)	$96\sqrt{2}$ r^3 = 356.80
Dx(g/cm^3)	4.424	5.370	5.140	4.903	

Orthopyroxene (Pbca)

	MgGeO$_3$[1]	CoGeO$_3$[6]	FeGeO$_3$	MnGeO$_3$[7]	ideal (r = 1.38 Å)[5]
a (Å)	18.829(3)	18.77		19.267(6)	$16\sqrt{6}$ r/3 = 18.028
b (Å)	8.952(2)	8.99		9.248(3)	6 r = 8.280
c (Å)	5.347(1)	5.35		5.477(2)	$2\sqrt{3}$ r = 4.781
a/b	1.9916	2.0879		2.0833	$32/6\sqrt{6}$ = 2.177
c/b	0.5972	0.5951		0.5922	$1/\sqrt{3}$ = 0.5774
V (Å^3)	901.26(3)	902.77		975.89	$192\sqrt{2}$ r^3 = 713.60
Dx(g/cm^3)	4.271	5.283		4.778	

1) present work. 2) Peacor (1968). 3) from our structure analysis which will be published elsewhere. 4) Hirano et al. (1980). 5) r indicates the ionic radius of oxygen and the value of r is from Shannon (1976). 6) Tauber et al. (1965). 7) Fang et al. (1969).

Fig. 4. Variation with temperature of the cell parameters and volume of clinopyroxene-type and orthopyroxene-type structures of MgGeO$_3$, marked by subscripts c and o, respectively.

following characteristics: Both mean distances GeA–O and GeB–O are slightly increased and so are the volumes of the corresponding tetrahedra of GeA and GeB. These features are more extreme in the B chain than in the A chain. The octahedral volume and bond distances show larger expansions for Mg2 than for Mg1. The O3A′–O3A–O3A″ angle in the A chain increases at high temperatures in the stable region, indicating a lessening of the kink in the chain; the expansion of the Mg2 octahedron stretches the A chain due to the presence of a shared edge O2–O3 between the Mg2 octahedron and the GeA tetrahedron. On the other hand, the O3B′–O3B–O3B″ angle of the B chain, which is similar to the chain in clino-MgGeO$_3$, does not change significantly with temperature.

Our attempts to perform structure analyses of ortho-MgGeO$_3$ at temperature higher than 1000°C were unsuccessful due to the sublimation of the sample during diffraction-intensity measurement.

The clino-to-ortho transition in MgGeO$_3$

In the field of silicate-pyroxene polymorphs, several possible models for the ortho-to-clino transition in pyroxene have been proposed by Brown et al. (1961), Sadanaga et al. (1969), Coe (1970), and Smyth (1974). Recently Sueno and
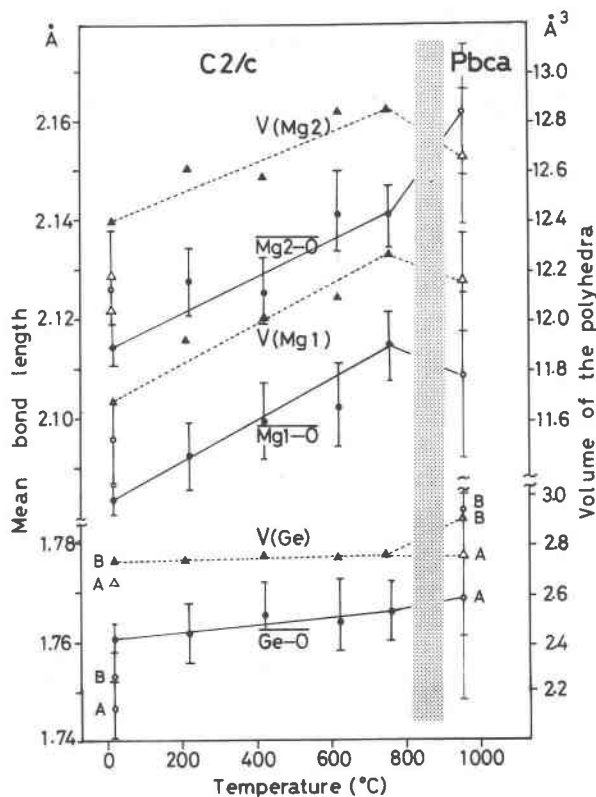

Fig. 5. Variation with temperature of mean bond lengths and polyhedral volumes of Mg1 and Mg2 octahedra and GeO$_4$ tetrahedron. Circlets and triangles, if solid, refer to the clinopyroxene-type structure; if open, to the orthopyroxene-type structure. Vertical line segments indicate the errors in the mean bond lengths.
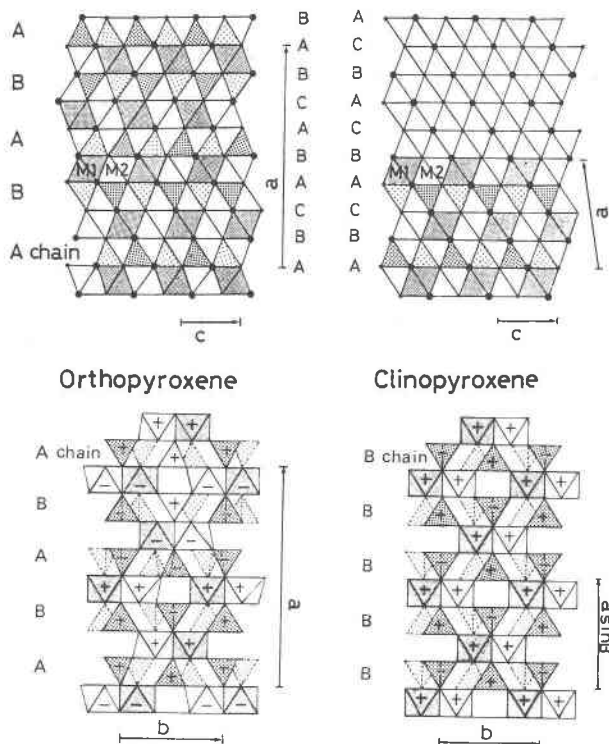
latter by Mg2 and two Ge's. The valence sum of these oxygens is $1\frac{2}{3}$ and $2\frac{1}{3}$, respectively. The different valence sums of these three oxygens are the cause of the different thermal expansion of the cation–oxygen bonds. The mean bond distances around the overcharged O3 atom show the largest thermal expansion and those around the undersaturated O2 have the smallest ones.

Bond strength is related to the force constant, which is derived from the frequency of the stretching mode of the thermal vibration. An anharmonic thermal vibration causing the thermal expansion is intensified by higher temperatures (Yamanaka et al., 1984). As a consequence, weaker bonds are easily excited, even by a small thermal energy, and they have the larger thermal expansion coefficient with increasing temperature. The above features of the thermal expansion were also found (by Smyth, 1973) in the orthopyroxene at high temperature up to 850°C.

The structure of ortho-MgGeO$_3$ at 950°C, in comparison with one quenched to room temperature, exhibits the

Fig. 6. Schematic diagrams of the clinopyroxene and orthopyroxene structures. Upper and lower figures are projections down **b** and **c**, respectively. Letters A, B and C denote the oxygen stacking layers. Symbols (+) and (−), after Papike et al. (1973), show orientation relationship between the basal triangles of the silicate tetrahedra and those of the octahedra to which the tetrahedra are attached.

hedra. Since Ge–O bonds have greater strength than M–O bonds, the GeO_4 tetrahedron can be regarded as a rigid body. Therefore Ge–O bonds do not break during the transition, while M–O bonds are broken by the shifting of the oxygen layers. The M1 and M2 octahedra in both the clino- and the ortho-$MgGeO_3$ are occupied by Mg; their volumes, therefore, are not extremely different in either structure. Consequently, a transition model including the cation movement may adequately represent the $MgGeO_3$ transition. The relationship between polymorphs is the same as in $MgSiO_3$ or $FeSiO_3$, whose structures have same cations in the M1 and M2 sites. The transition model in these structures was proposed by Brown et al. (1961), Sadanaga et al. (1969), Smyth (1974) and Sueno and Prewitt (1984).

Since the transition under consideration is topotactic and does not alter the crystal shape, the structural changes can result from a cooperative slip of oxygen layers by thermal shear stress, such as the one demonstrated by Takéuchi and Haga (1971).

We do not yet understand why the temperature dependence of $MgGeO_3$ polymorphs is different from that of silicate pyroxenes. Thermodynamic data on the stability relations between the two polymorphs of $MgGeO_3$, contrasting with those of silicate pyroxenes, would greatly enhance our comprehension of the transition mechanism and also increase our understanding of the pyroxene polymorphs.

Acknowledgments

References

Brown, W. L., Morimoto, N., and Smith, J. V. (1961) A structure explanation of polymorphism and transitions of MgSiO₃. Journal of Geology, 69, 609–616.

Cameron, M., Sueno, S., Prewitt, C. T., and Papike, J. J. (1973) High temperature crystal chemistry of acmite, diopside, hedenbergite, jadeite, spodumene and ureyite. American Mineralogist, 58, 594–618.

Coe, R. S. (1970) The thermodynamic effects of shear stress on the ortho-clino inversion in enstatite and other coherent phase transition characterized by a finite simple shear. Contribution to Mineralogy and Petrology, 26, 247–264.

Coe, R. S. and Müller, W. F. (1973) Crystallographic orientation of clinoenstatite produced by deformation of orthoenstatite. Science, 180, 64–66.

Coppence, P. and Hamilton, W. C. (1970) Anisotropic extinction corrections in the Zachariasen approximation. Acta Crystallographica, A26, 71–83.

Fang, J. H., Townes, W. D., and Robinson, P. D. (1969) The crystal structure of manganese metagermanate MnGeO₃. Zeitschrift für Kristallographie, 130, 139–147.

Grebenshchikov, R. G., Motsartov, V. V., and Chigareva, O. G. (1976) Solid solutions in the Ca₀.₅Mg₀.₅GeO₃–FeGeO₃ system. Russian Journal of Inorganic Chemistry, 21, 1368–1370.

Prewitt (1984) reviewed these models and presented a new one for the transition from orthoferrosilite to high-clinoferrosilite. Many papers have discussed the ortho-to-clino transition in enstatite caused by shear stress on (100) in the [001] direction, from observation made by electron microscopy (Coe and Müller, 1973; Kirby, 1976).

In this paper we have presented a new type of transition in pyroxene-type structures, viz. a clino-to-ortho transition at elevated temperature. This transition is the reverse of that observed in silicate pyroxenes. In both clino- and ortho-$MgGeO_3$ structures, tetrahedral and octahedral layers are alternately stacked along the **a** axis (Figs. 2 and 3). The clino-to-ortho transition requires the following rearrangements: (1) The octahedral stacking sequence, in the notation of Papike et al. (1973), changes from $(+ \ +)_\infty$ in the clino to $(+ \ + \ - \ -)_\infty$ in the ortho; (2) The running direction of the basal triangle of the tetrahedra changes from $(+ \ -)_\infty$ to $(+ \ + \ - \ -)_\infty$ in the order of the tetrahedral stacking layers along [100]; (3) The stacking layers in the clino, composed of oxygen atoms in CCP, (ABCABC ...) shift to $(ABCABACB)_\infty$ in the ortho by slip of oxygen layers with a magnitude of $c/3$ or $-2c/3$ (Fig. 6).

All oxygens are shared with silicate chains and octa-

Hirano, M., Tokonami, M., and Morimoto, N. (1980) Crystal-chemistry of MnGeO$_3$ polymorphs. Journal of Mineralogical Society of Japan, 14, 158–164.

Kirby, S. H. (1976) The role of crystal defects in the shear-induced transformation of orthoenstatite to clinoenstatite. In H. R. Wenk et al. (Eds.) Electron microscopy in Mineralogy, p. 465–472. Springer-Verlag, Berlin, Heidelberg.

Murakami, T., Takéuchi, Y., and Yamanaka, T. (1982) The transition of orthoenstatite to protoenstatite and the structure at 1080°C. Zeitschrift für Kristallographie, 160, 292–312.

Ozima, M. and Akimoto, S. (1983) Flux growth of single crystals of MgGeO$_3$ polymorphs (orthopyroxene, clinopyroxene, and ilumenite) and their phase relations and crystal structures. American Mineralogist, 68, 1199–1205.

Papike, J. J., Prewitt, C. T., Sueno, S., and Cameron, M. (1973) Pyroxene: comparisons of real and ideal structural topologies. Zeitschrift für Kristallographie, 138, 258–273.

Peacor, D. R. (1968) The crystal structure of CoGeO$_3$. Zeitschrift für Kristallographie, 126, 299–306.

Ringwood, A. E. and Seabrook, M. (1963) High pressure phase transformations in germanate pyroxenes and related compounds. Journal of Geophysical Research, 68, 4601–4609.

Robbins, C. R. and Levin, E. M. (1959) The system magnesium oxide-germanium dioxide. American Journal of Science, 257, 63–70.

Roth, R. S. (1955) Synthetic alkaline earth germanates isostructural with enstatite and pseudowollastonite. American Mineralogist, 40, 332.

Royan, P. and Forwerg, W. (1963) Darstellung und Eigenschaften der Metagermanate MnGeO$_3$, FeGeO$_3$ und CoGeO$_3$. Naturwissenschaften, 50, 41.

Sadanaga, R., Okamura, F. P., and Takeda, H. (1969) X-ray study of the phase transformations of enstatite. Mineralogical Journal, 6, 110–130.

Shannon, R. D. (1976) Residual effective ionic radii and systematic studies of interatomic distances in halides and chalcogenides. Acta Crystallographica, A32, 751–767.

Smith, J. V. (1969) Crystal structure and stability of the MgSiO$_3$ polymorphs: physical properties and phase relations of Mg, Fe pyroxenes. Mineralogical Society of America. Spec. Pap., 2, 3–29.

Smyth, J. R. (1973) An orthopyroxene structure up to 850°C. American Mineralogist, 58, 636–648.

Smyth, J. R. (1974) Experimental study on the polymorphism of enstatite. American Mineralogist, 59, 345–352.

Sueno, S. and Prewitt, C. T. (1984) Models for the phase transition between orthoferrosilite and high clinoferrosilite. Fortschritte der Mineralogie, 61, 223–241.

Takéuchi, Y. and Haga, N. (1971) Structural transformation of trioctahedral sheet silicate. Mineralogical Society of Japan, Spec. Pap. 1, 74–87.

Tauber, A., Kohn, J. A., Whinfrey, C. G., and Babbage, W. D. (1963) The occurrence of an enstatite phase in the subsystem GeO$_2$–MnGeO$_3$. American Mineralogist, 48, 555–565.

Tauber, A. and Kohn, J. A. (1965) Orthopyroxene and clinopyroxene polymorphs of CoGeO$_3$. American Mineralogist, 50, 13–21.

Thompson, J. B. (1970) Geometrical possibilities for amphibole structures model biopyriboles. American Mineralogist, 55, 292–293.

Yamanaka, T., Takéuchi, Y., and Sadanaga, R. (1981) Gas-flame, high temperature apparatus for single-crystal X-ray diffraction studies. Zeitschrift für Kristallographie, 154, 147–153.

Yamanaka, T., Takéuchi, Y., and Tokonami, M. (1984) Anharmonic thermal vibrations of atoms in MgAl$_2$O$_4$ spinel at temperatures up to 1933°K. Acta Crystallographica, B40, 96–112.